# Hybrid Method for Analysis and Design of Slope Stabilizing Piles

R. Kourkoulis[1]; F. Gelagoti[2]; I. Anastasopoulos[3]; and G. Gazetas, M.ASCE[4]

**Abstract:** Piles are extensively used as a means of slope stabilization. Despite the rapid advances in computing and software power, the design of such piles may still include a high degree of conservatism, stemming from the use of simplified, easy-to-apply methodologies. This paper develops a hybrid method for designing slope-stabilizing piles, combining the accuracy of rigorous three-dimensional (3D) finite-element (FE) simulation with the simplicity of widely accepted analytical techniques. It consists of two steps: (1) evaluation of the lateral resisting force (*RF*) needed to increase the safety factor of the precarious slope to the desired value, and (2) estimation of the optimum pile configuration that offers the required *RF* for a prescribed deformation level. The first step utilizes the results of conventional slope-stability analysis. A novel approach is proposed for the second step. This consists of decoupling the slope geometry from the computation of pile lateral capacity, which allows numerical simulation of only a limited region of soil around the piles. A comprehensive validation is presented against published experimental, field, and theoretical results from fully coupled 3D nonlinear FE analyses. The proposed method provides a useful, computationally efficient tool for parametric analyses and design of slope-stabilizing piles. **DOI: 10.1061/(ASCE)GT.1943-5606.0000546.** © *2012 American Society of Civil Engineers.*

**CE Database subject headings:** Slope stability; Soil-structure interactions; Pile groups; Validation; Experimentation; Field tests; Hybrid methods.

**Author keywords:** Slope stability; Soil-structure interaction; Pile groups; Validation against experiments; Simplified method; Field tests.

## Introduction

Installing dowelling piles is an effective technique for improving the stability of precarious slopes, because they can be easily constructed without disturbing the equilibrium of the slope. Many successful applications of pile-stabilization techniques have been reported in the literature. Among the oldest references are De Beer and Walleys (1972), Ito and Matsui (1975), Sommer (1977), Fukuoka (1977), D'Appolonia et al. (1997), Wang et al. (1979), and Nethero (1982). Examples of piles stabilizing slopes on which structures are to be founded include landing piers in harbors (Kitazima and Kishi 1967; Leussink and Wenz 1969; De Beer and Wallays 1972), bridge abutments (Nicu et al. 1971), and buildings (Heyman and Boersma 1961). The utilized pile types range from timber to cast-in-place and steel-tube piles.

Piles used in slope stabilization are subjected to lateral forces by horizontal movements of the surrounding soil, and are hence regarded by researchers as passive piles (Viggiani 1981; Poulos 1995; Hassiotis et al. 1997). Several empirical, analytical, and numerical methods to design stabilizing piles exist. Broadly, these methods can be classified in two types: (1) pressure or displacement-based methods (De Beer et al. 1972; Tschebotarioff 1973; Ito and Matsui 1975; Hassiotis et al. 1997; Poulos 1995; Chen et al. 1997), and (2) numerical methods, such as finite elements and finite differences (Oakland and Chameaou 1984; Goh et al. 1997; Poulos and Chen 1997).

### Pressure or Displacement–Based Methods

In these methods, the pile is modeled as a beam connected with the soil through nonlinear springs, at the support of which the displacement of the slope is imposed. Hence the assessment of pile lateral capacity is accomplished by solving two differential equations:

1. For the portion of pile above the sliding surface:

$$EI\left(\frac{d^4y_1}{dz^4}\right) = q(z), \quad \text{for } z < 0 \tag{1}$$

in which $y_1$ = pile deflection above the sliding surface (assumed to lie at $z = 0$) and $EI$ = pile stiffness. The force intensity, $q(z)$, is calculated using the principle of plastic deformation of soil.

2. For the portion of pile below the sliding surface:

$$EI\left(\frac{d^4y_2}{dz^4}\right) = -Ky_2, \quad \text{for } z \geq 0 \tag{2}$$

where $y_2$ = pile deflection below the sliding surface and $K$ is related to the modulus of subgrade reaction of soil.

Despite its simplicity, this approach requires predetermining the slope-displacement profile and the distribution of lateral soil modulus (the assessment of which may require extensive field measurements), as well as the limiting lateral pile-soil pressure with depth. A number of analytical approaches have been developed for the determination of the latter.

Among the most widely accepted are the approaches of Poulos (1973, 1999), Viggiani (1981), and Reese et al. (1992). These

[1]Postdoctoral Researcher, Soil Mechanics Laboratory, National Technical Univ. of Athens, Athens, Greece.

[2]Postdoctoral Researcher, Soil Mechanics Laboratory, National Technical Univ. of Athens, Athens, Greece.

[3]Adjunct Lecturer, National Technical Univ., Athens, Greece.

[4]Prof. of Civil Engineering, National Technical Univ., Athens, Greece (corresponding author). E-mail: gazetas@central.ntua.gr

Note. This manuscript was submitted on December 20, 2009; approved on April 5, 2011; published online on April 7, 2011. Discussion period open until June 1, 2012; separate discussions must be submitted for individual papers. This paper is part of the ***Journal of Geotechnical and Geoenvironmental Engineering***, Vol. 138, No. 1, January 1, 2012. ©ASCE, ISSN 1090-0241/2012/1-1–14/$25.00.

methods assume a single laterally loaded pile and correlate the ultimate soil-pile resistance with the undrained shear strength for clays, and with the overburden stress and friction angle for sands. A drawback of these methods is that group effects are simplistically taken into account by the application of reduction factors (e.g., Chen and Poulos 1993; Poulos 1995; Guerpillon et al. 1999; Jeong et al. 2003).

Ito and Matsui (1975) developed a plastic extrusion-deformation model for rigid piles of infinite length (and not closely spaced) to estimate the shear resistance offered by a row of piles embedded in a slope. Their approach presumes that the soil is soft and deforms plastically around piles. Despite its rigor, the method neglects pile flexibility, pile limited length, and soil arching—phenomena that may all have a substantial effect (Zeng and Liang 2002; Liang and Yamin 2009). This approach has formed the basis of a number of design methods (Popescu 1991; Hassiotis et al. 1997).

### Numerical Methods

Because of the dramatic progress in computing and software power over the last few years, the finite-element (FE) and finite-difference (FD) methods are increasingly popular. These methods provide the ability to model complex geometries and soil-structure interaction phenomena such as pile-group effects. Moreover, they are able to model the three dimensionality of the problem, and may well capture soil and pile nonlinearities.

As early as 1979, Rowe and Poulos (1979) developed a two-dimensional (2D) finite-element approach that, in a simplified way, accounted for the three-dimensional (3D) effect of soil flowing through rows of piles. A 3D elastic FE approach has been developed by Oakland and Chameau (1984) for the analysis of stabilization of surcharged slopes with drilled piles.

Chow (1996) presented a numerical model in which the piles are modeled using beam elements and the soil is modeled using a hybrid method of analysis, which simulates the soil response at individual piles (using the subgrade reaction modulus) and the pile-soil-pile interaction (using the theory of elasticity). This method has been recently used by Cai and Ugai (2000) to analyze the effect of piles on slope stability.

More recently, Kim et al. (2002) introduced a model based on the load-transfer approach to compute the load and deformations of piles subjected to lateral soil movement.

Despite their potential rigor, the application of numerical methods in three dimensions requires extensive computational resources, often becoming unattractive to practitioners. Therefore, this paper presents and validates a hybrid methodology for the design of slope-stabilizing piles, combining the accuracy of rigorous 3D FE simulation with the simplicity of widely accepted analytical techniques. The proposed methodology is further exploited in Kourkoulis et al. (2011) to gain insight into the factors affecting the response and to produce design charts for slope-stabilization piles that can be useful in practice.

## Fundamentals of the Proposed Procedure

The problem investigated in this paper is shown in Fig. 1. A row of slope-stabilizing piles is embedded in the slope that is prone to failure. The upper soil layer, called unstable soil, overlies the stable soil layer. Sandwiched between these two layers lies the potential sliding interface. The presence of the piles enhances the stability of the slope. On the other hand, the pile reacts to the movement of the unstable soil through deformation, which in turn causes pile stressing.

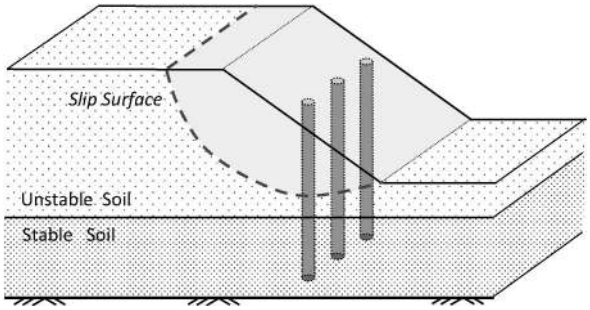


**Fig. 1.** Problem definition: a row of stabilizing piles embedded within a slope that is prone to failure

The two issues are interrelated: the increase in slope stability depends on the amount of shear force that can be developed by the pile at the level of the sliding plane, whereas the position of the sliding plane determines the shear force developed on the pile (Poulos 1999).

The general design procedure adopted by the present study follows the well-documented decoupled approach described by Viggiani (1981), Hull (1993), and Poulos (1995, 1999), and consists of two main steps [see also the conceptual diagram of Fig. 2; created following Poulos (1999)]. It is as follows:

1. Step 1: Evaluation of the total shear force needed to increase the safety factor of the slope to the desired value (based on analysis of the unreinforced slope).
2. Step 2: Estimation of the optimum pile configuration offering the required $RF$ for a prescribed deformation level.

Step 1 utilizes the results of conventional slope-stability analysis and may be readily applied by engineering practitioners. A novel approach is presented in this paper for calculation of pile lateral capacity (Step 2) that aims at reducing the amount of computational effort normally associated with rigorous 3D soil-structure interaction analyses.

### Step-by-Step Description of the Proposed Methodology

The proposed methodology is schematically illustrated in Fig. 3. An existing slope is considered as having an actual factor of safety ($SF$) that must be increased through pile inclusion to a greater target value $SF_T$. The two steps are as follows:

**Step 1: Calculation of Required Lateral Resisting Force to Be Offered by Piles.** During this step [Fig. 3(a)], the driving ($F_D$) and resisting ($F_R$) forces along the slip surface are calculated using one of the widely accepted slope-stability analysis techniques (e.g., Sarma, Spencer, Bishop, or Janbu). Most of these methods

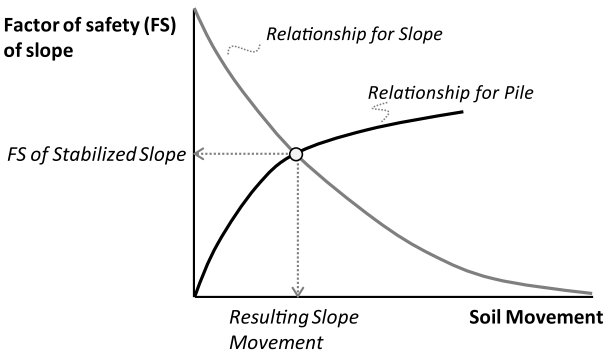


**Fig. 2.** Conceptual approach for estimating slope movement after stabilization (data from Poulos 1999)

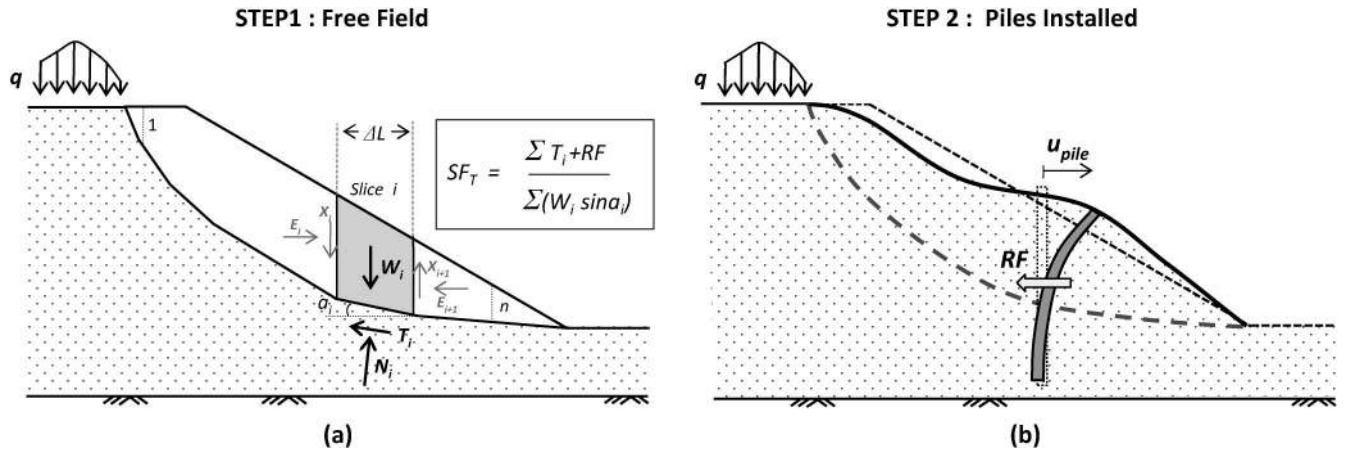


**Fig. 3.** Schematic illustration of the two steps of the decoupled methodology: (a) limit equilibrium slope-stability analysis to compute the additional required resistance force *RF*; (b) estimate pile configuration capable of providing the required *RF* at prescribed displacement

divide the sliding wedge into slices and integrate the forces along each slice to obtain the total driving and resisting forces.

If the actual safety factor, *SF*, is less than the target safety factor, $SF_T$, the piles must provide an additional resistance force, *RF*, so that

$$SF_T = \frac{\sum F_R + RF}{F_D} \tag{3}$$

The adoption of the conventional limit-equilibrium calculation of the driving and resisting forces is, of course, leading to a conservative estimate of the required pile resistance force. This decoupled approach tacitly assumes that the position of the sliding surface is not affected by the very presence of the piles. This means that geometry-dependent phenomena such as the effect of soil arching (Liang and Yamin 2009) in the area of the piles (which may reduce soil movement) are conservatively ignored in the calculation of the required pile, *RF*. Such effects, however, will be captured by the numerical analysis involved in the second step of the method.

**Step 2: Estimation of Pile Configuration to Provide the Required RF at Acceptable Deflection.** For the second step [Fig. 3(b)], a reasonable procedure is to analyze the pile subjected to lateral soil movement, simulating the movement of the sliding mass. The lateral capacity of the stabilization piles to such movements may be rigorously assessed using the FE technique, which provides the ability to model the whole 3D geometry. However, a complete analysis of the full geometry model may be computationally inefficient (especially when multiple parametric analyses are required) for the following reasons:

1. Although the required pile resistance force is indeed a function of slope geometry, its calculation has already been incorporated in the slope-stability analysis of Step 1. The ultimate pile load that is sought at this stage depends primarily on the depth of the interface and the mechanical properties (strength) of soil.
2. Pile loading (independently of the slope inclination and interface position) stems from the application of an almost uniform displacement profile along the pile length in the unstable soil.

The reasonable validity of uniformity of the displacement distribution has been proposed by Poulos (1999) and verified in Kourkoulis (2009) as an appealing simplification to the slope displacements applied on the pile. Following Poulos (1999), the displacement imposed on the piles by the sliding wedge can be assumed to be uniformly distributed with depth within the sliding block, reducing linearly to zero within the shear band.

The research presented in this paper examines only piles located in the middle part of the sliding mass. The validity of the assumption of displacement uniformity at a distance of 5*D* (where *D* is the pile diameter) for piles located near the toe or the crest of the slope has not been investigated. An adequate number of FE analyses were performed to confirm the selection of 5*D* as the distance beyond which the soil displacement may be considered as uniform, i.e., unaffected by the presence of the piles. These analyses involved piles located in the middle of the slope in a homogeneous soil, varying the soil properties, slope inclination, landslide depth, and pile spacing. The example geometries are displayed in Table 1. Typical results are presented in Fig. 4(a) in terms of horizontal displacement contours. The soil-displacement profile along vertical cross sections at a distance of 5*D* upslope of the piles as calculated by fully coupled 3D finite-element analyses for several slope geometries is presented in Fig. 4(b), The displacement is maximum at the top, decreasing by no more than 15% just above the sliding interface. Hence, within engineering accuracy, at 5*D* distance (i.e., at the boundary of the simplified model at which the imposed displacement is to be applied) the distribution of soil displacement with depth can indeed be approximated as uniform.

Taking this into account, this study proposes a simplified methodology for calculation of pile lateral capacity (i.e., the ultimate pile resistance), decoupling it from the slope geometry [the effect of which has already been included in the calculation of the demand (i.e., the required lateral resisting force) in Step 1].

**Table 1.** Summary of Slope Characteristics (Geometry and Sliding Interface Properties) and Pile Configurations Analyzed through Fully Coupled 3D FE Analysis

| Slope inclination ($\beta$°) | Interface depth (m) | Pile-to-pile distance |
|---|---|---|
| Residual interface strength properties: $\varphi = 19°$, $c = 3$ kPa | | |
| 24 | −8 | 2*D* |
| | | 3*D* |
| Residual interface strength properties: $\varphi = 16°$, $c = 3$ kPa | | |
| 22 | −6 | 2*D* |
| | | 3*D* |
| Residual interface strength properties: $\varphi = 14°$, $c = 3$ kPa | | |
| 20 | −4 | 2*D* |
| | | 3*D* |

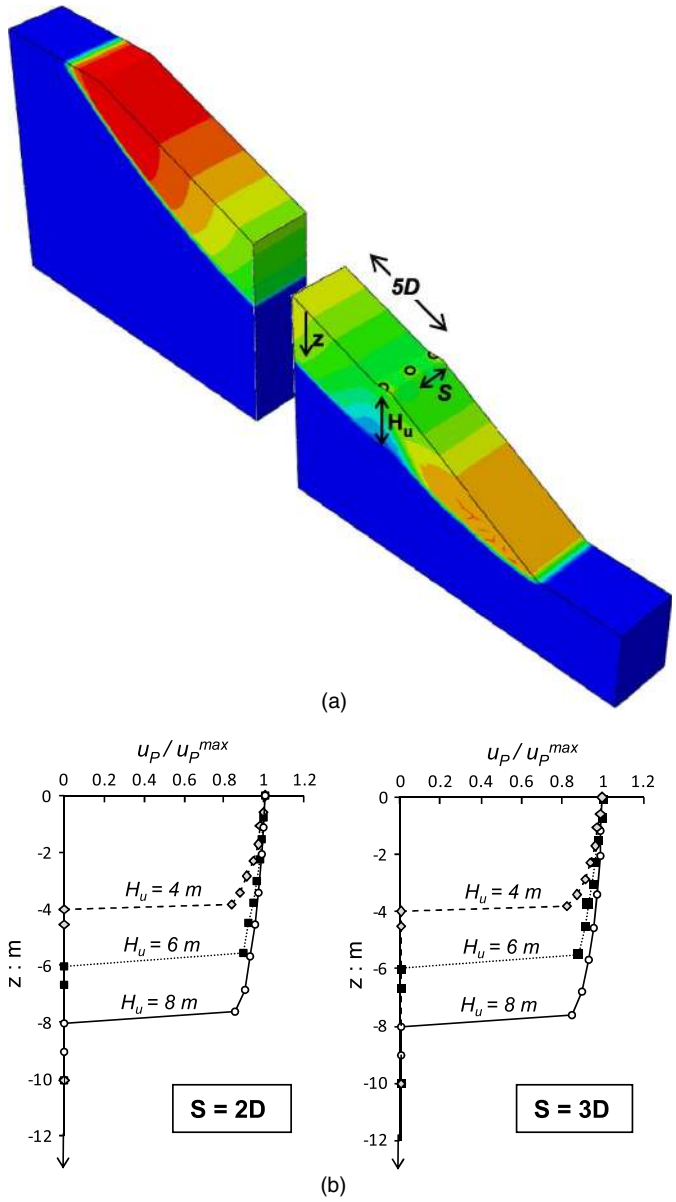


**Fig. 4.** Illustration of the validity of the assumption of a practically uniform soil-displacement profile at a distance of five diameters upslope of the piles: (a) contours of horizontal soil displacements for an example case of a 6-m-depth slide; (b) distribution of soil displacement with depth within the sliding wedge for all examined slide depths and pile spacings resulting from the coupled 3D FE analyses

The following section highlights the proposed simplified methodology.

## Simplified Methodology for Estimation of Pile Ultimate Resistance

The primary concept of the simplified methodology for estimation of pile ultimate resistance is schematically shown in Fig. 5. Instead of modeling the whole slope-soil-pile system, the focus is on the pile and the soil at its immediate vicinity. Modeling only a representative region of soil around the pile, the ultimate resistance is computed by imposing a uniform displacement profile onto the model boundary. Although the actual magnitude of the imposed displacement will indeed depend on slope geometry, the ultimate load (sought at this stage) only requires that the applied displacement be large enough to mobilize the lateral capacity of the soil-pile system. This simplified decoupled approach is considered quite realistic in the case of preexisting sliding planes within the soil mass, at which point the position of the interface will not be modified by the presence of the piles. It is assumed that the slope-failure surface preexists, having been generated during a previous event that caused strength mobilization along a well-defined continuous surface. This type of landslide (i.e., sliding along a preexisting interface) has been demonstrated by many researchers (e.g., Ambrasseys and Srbulov 1995; Tika-Vassilikos et al. 1993; Chandler 1984; Gazetas and Uddin 1994) as being characteristic of several actual observed slope failures.

The optimum pile location along the slope has not been investigated. It is recommended that the piles are placed in the middle part of the slope provided that the soil block downslope of the piles is stable. In this case, following Yamin and Liang (2009) the optimal pile location is indeed located in the middle of the slope.

### Geometry of the Simplified Model

The model shown in Fig. 5 contains two piles of diameter $D$ and length $L_p$. Having eliminated slope geometry, a sliding interface (representing the sliding plane of the moving slope) is incorporated in the FE model at depth $H_u$; the piles are embedded in the stable soil by the length $L_E$. Because the zone of influence of each pile has been demonstrated (e.g., Reese and Van Impe 2001) not to exceed $5D$, the length of the model is restricted to $10D$. The model width, on the other hand, is a function of pile spacing: the FE model represents a typical slice of the slope stabilized with piles spaced at distance $S$, which is assumed to be repeated indefinitely in the $y$-direction. Consequently, the width of the model is equal to $2S$. Symmetry conditions are applied at its front and rear sides, restraining movement along the $y$-direction but allowing vertical and horizontal displacements. Vertical and horizontal displacement at the base nodes of the model is, of course, constrained. The fixity of the pile into the stable layer would depend on its embedment depth and on the strength of the stable layer. No artificial boundary condition is imposed on the pile. Analyses were conducted using the FE code ABAQUS (ABAQUS FEA).

### Modeling of Soil and Pile

Figs. 6 and 7 illustrate the 3D discretization into finite elements and some aspects of pile modeling. An elastoplastic constitutive model with Mohr-Coulomb failure criterion is used for the soil (Fig. 6), whereas the pile is modeled with 3D beam elements circumscribed by eight-noded hexahedral continuum elements of nearly zero stiffness (Fig. 7). The pile stiffness is introduced in the simulation through the central beam element, the nodes of which are rigidly connected with the circumferential solid-element nodes at the same height. Consequently, each pile section behaves as a rigid disk: rotation is allowed on the condition that the disk remains perpendicular to the beam axis, but stretching cannot occur. This technique allows the calculation of the pile internal forces directly from the beam elements; at the same time, 3D geometry effects are indeed captured because of the presence of the circumferential solid elements. Sliding and detachment of the pile from the surrounding soil can be captured through interface elements placed at the pile periphery. In the analyses presented in this paper, full bonding conditions have been assumed. However, the investigated problem is not so sensitive to the properties of the interface (the response is primarily controlled by passive soil resistance).

Both elastic and inelastic pile behavior is modeled. For the latter case, knowledge of the moment-curvature relationship ($M - \theta$) of the pile cross section is required. For the nonlinear pile analyses

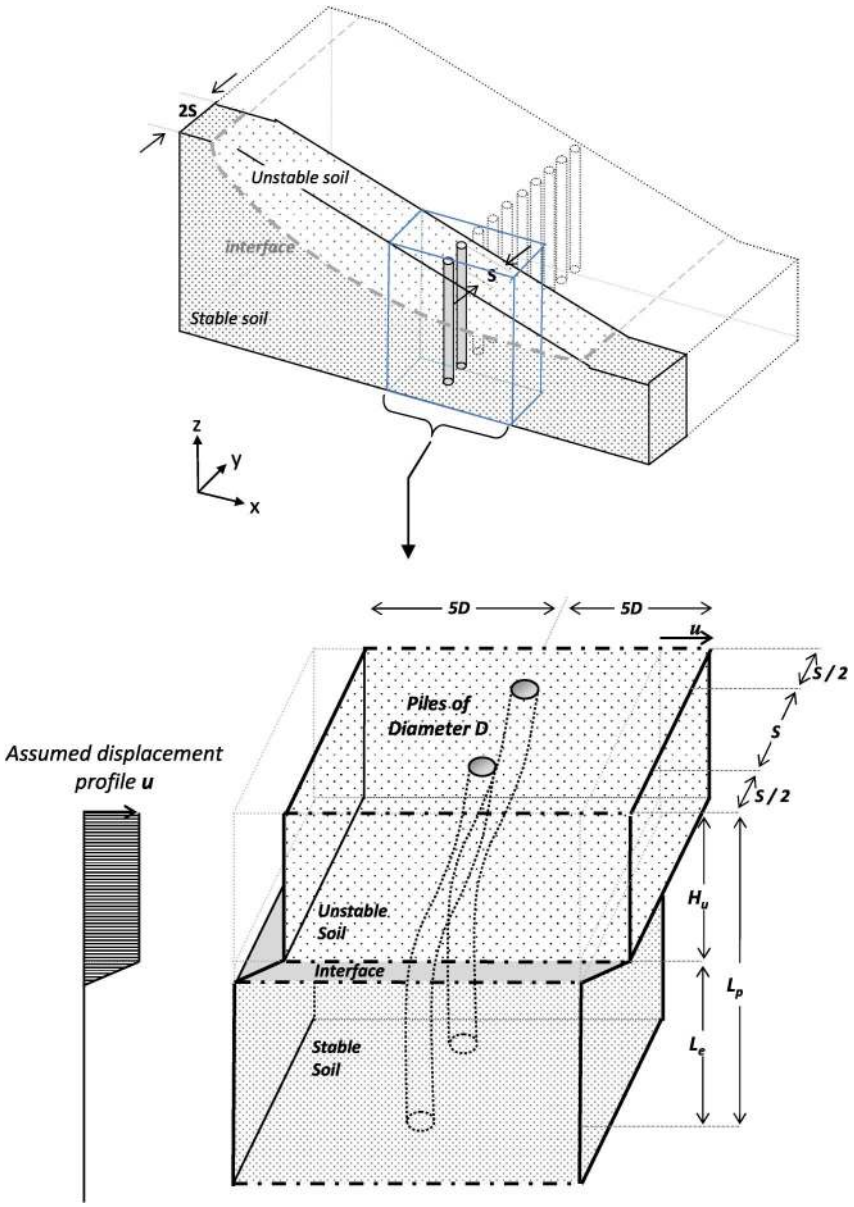


**Fig. 5.** Schematic illustration of the simplified decoupled methodology for estimation of pile ultimate resistance; instead of modeling the whole slope-soil-pile system (top sketch), the focus is on the pile and a representative region of soil at its immediate vicinity (boxed area); the geometry and key parameters of the simplified model are shown in the bottom sketch

presented here, a perfectly plastic behavior is assumed; i.e., pile strength resistance is constant after reaching its ultimate capacity. Strength degradation beyond this point has not been taken into account.

### *Calculation of Ultimate Pile Resistance Force*

The displacement is applied simultaneously on all side nodes (located at distance of 5*D* from the piles) of the upper part (unstable layer) of the model, progressively increasing incrementally until the failure of the piles. The FE analysis provides the reaction force at the nodes at which the displacement is applied. The sum of these forces is the total reaction force, $RF_{\text{total}}$, which reflects both the resistance from the piles and the shear resistance of the soil itself (within the sliding interface). Hence, to extract the net resistance of the piles, the free-field problem is analyzed first (i.e., same model but without piles), yielding the free-field reaction force $RF_{\text{FF}}$. The latter is subtracted from the total reaction force, $RF_{\text{total}}$, to yield the net reaction force of the piles $RF_{\text{pile}}$ (Fig. 8). Hence, the accuracy in estimation of the sliding interface properties (cohesion $c_o$ and friction angle $\varphi_o$) play a trivial role in determining the pile lateral load, given that the shear strength along the interface is substantially less than the strength of overlying ($c_1$, $\varphi_1$) and underlying ($c_2$, $\varphi_2$) soils.

The methodology described previously may be used to provide design charts for the estimation of $RF_{\text{pile}}$ for rows of piles at various spacings, nailing precarious slopes of any depth. The full 3D FE calculations provide the evolution of *RF* with pile-deflection and pile-bending moment, as well as with the displacement of the soil between two consecutive piles of the row (indication of arching). An example design chart is provided in Fig. 9. The chart gives the *RF* offered by three different pile configurations, nailing a slide of a moderate 6-m depth. The stable soil layer in this case is modeled as very stiff and the pile as adequately long, so that fixity conditions are guaranteed immediately below the interface. For a specific level of *RF*, several pile configurations may be able to offer the required *RF*, but for different displacement levels. It is up to the designer to

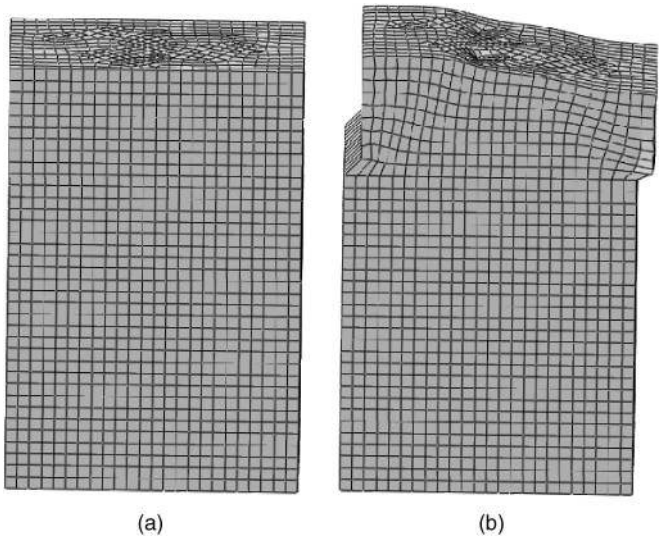


**Fig. 6.** Finite-element discretization of the proposed simplified decoupled model: (a) undeformed mesh; (b) deformed mesh after application of the imposed uniform lateral displacement

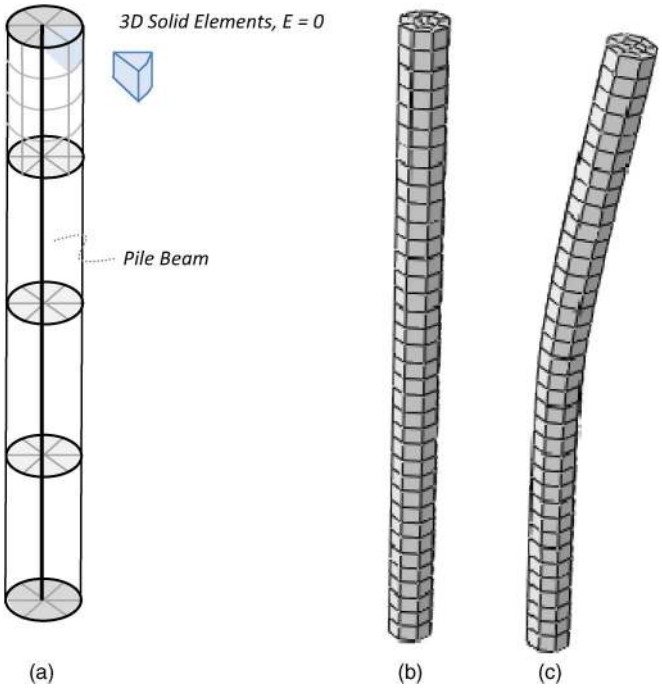


**Fig. 7.** (a) Schematic illustration of pile modeling; (b) pile FE discretization; (c) deformed pile after application of the imposed deformation

specify the acceptable displacement of the pile and the soil, and to thereby choose an optimal configuration. Several design charts for various soil and slide conditions, as well as insight into the various factors affecting the behavior of slope-stabilizing piles (such as pile length, embedment depth, and soil inhomogeneity) are presented and discussed by Kourkoulis et al. (2011).

Geometry-dependent phenomena such as soil arching, which had been neglected during the first step of the method, are inherently captured by the 3D numerical analyses. Therefore, the design charts refer to piles spaced between two and four times their diameter so that arching can develop.

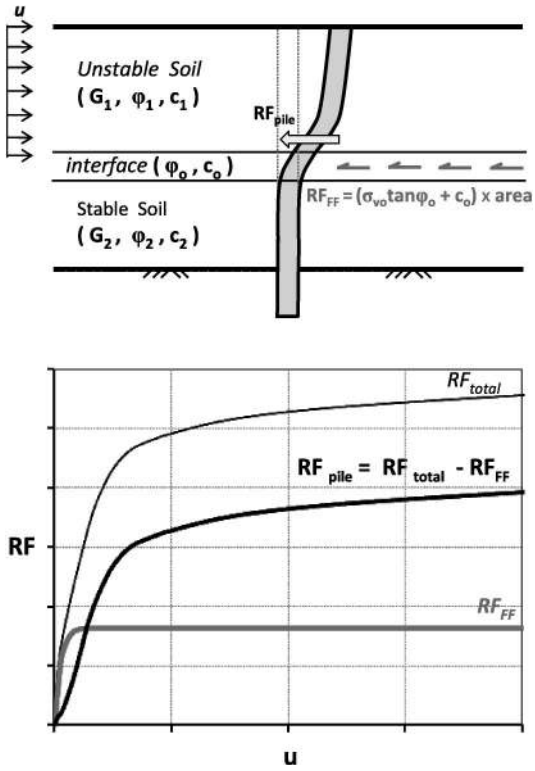


**Fig. 8.** Calculation of net pile resistance force $RF_{\text{pile}}$ against imposed displacement $u$; the free-field reaction force $RF_{FF}$ caused by mobilization of shear strength at the interface is subtracted from the total reaction force $RF_{\text{total}}$

## Validation of the Numerical Analysis Methodology

The effectiveness of the proposed hybrid methodology for the design of slope-stabilizing piles largely relies on the validity of the numerical analysis method employed. Making use of published experimental, field, and theoretical results, this section validates the numerical analysis methodology against the following:

1. A 16-year-long case history (Frank and Pouget 2008) of a pile embedded in a creeping slope with a preexisting potential sliding interface. A coupled numerical simulation has been performed to predict the recorded evolution of soil deformation and pile deflection, and
2. Widely accepted theoretical solutions.

Further validation of the numerical model against centrifuge model tests of flexible steel piles in sand and a 1-*g* pushover test of a rigid pile in sand can be found in Kourkoulis (2009).

As will be shown, the FE model employed is capable of reproducing the results of all tests with no need for further calibration of its parameters, provided that both pile and soil properties are reliably known. The validated coupled numerical procedure will be used in the following to investigate the accuracy of the decoupled methodology.

### *Validation against a Long-Term Ful-Scale Field Test: Case History of Pile Subjected to Slope Movement*

**Experimental Site of Salledes.** This unique 16-year field experiment, recently documented and evaluated by Frank and Pouget (2008), refers to a site in Salledes, France, of 7% surface inclination and composed of 5–8 m thick colluvial marls, which slowly (in a creeping fashion) slides on the interface with a marly compact Oligocene substratum (Fig. 10). In 1980, an embankment was constructed and a steel pipe pile of 12-m length was installed at 7.5-m

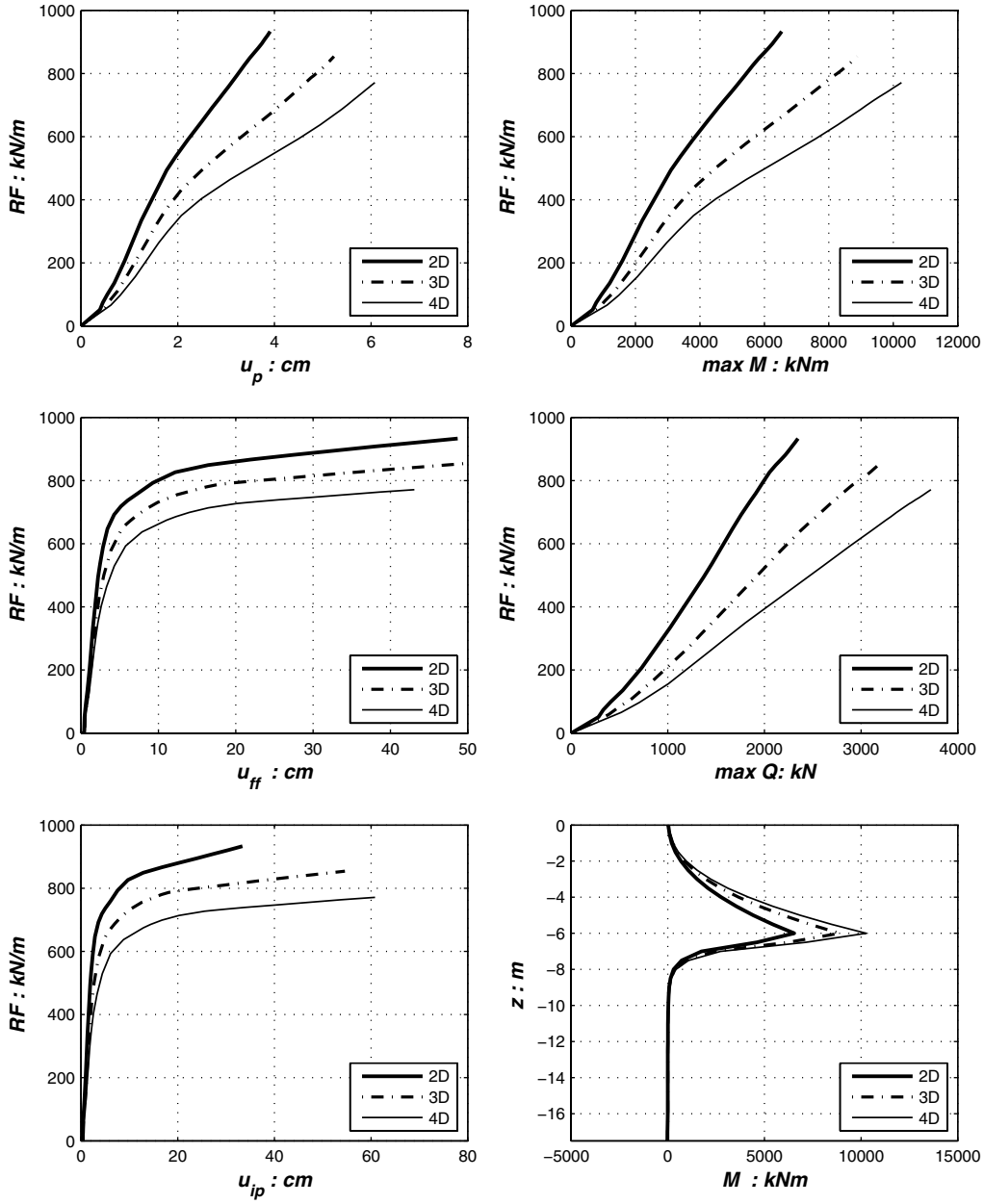


**Fig. 9.** Example of a design chart; unstable soil characteristics: linearly varying with depth soil profile ($G = 40$ MPa, $\varphi = 28°$, $c = 1$ kPa, $H_u = 6$ m); stable soil characteristics: stiff rock ($G = 4$ GPa, $\varphi = 45°$, $c = 100$ kPa) pile characteristics ($D = 1.2$ m, $L_E = H_u$), elastic pile

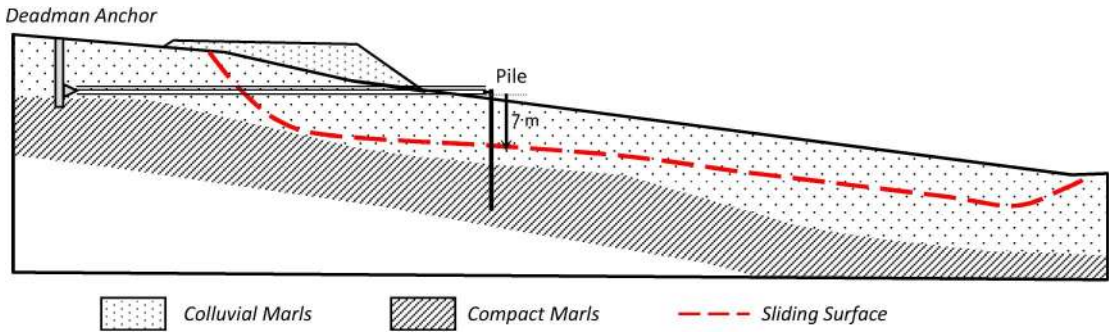


**Fig. 10.** Long-term full-scale field test by Frank and Pouget (2008): geological section; the pile is connected to a deadman anchor 39 m upslope to set pile-head displacement to zero

distance downslope of the toe of the embankment. At this location, the sliding interface lies at 6.2-m depth and the compact marls at approximately 7-m depth. The soil profile shows a moderately high undrained shear strength ranging from 50 to 120 kPa. Several Menard and self-boring pressuremeter tests were conducted to estimate soil stiffness. The main characteristics of the steel pile are as follows: total length = 12 m; embedded length = 11 m; external diameter $D = 0.915$ m; wall thickness $t = 19$ mm; and flexural stiffness $EI = 1.07$ GN m$^2$.

To achieve the maximum relative displacement between the sliding soil wedge and the pile, a zero-displacement condition was pursued for the pile head. For this purpose, the pile head was connected to a deadman anchor located 39 m upslope. However, because of parasitic movements stemming from its creeping anchoring system, the pile head had to be pulled back to its original position several times during the 16 years of the experiment.

The displacement time history of the free field is chronicled in Fig. 11(a), and the evolution of the force applied at the pile head is plotted in Fig. 11(b), showing a seesawing behavior.

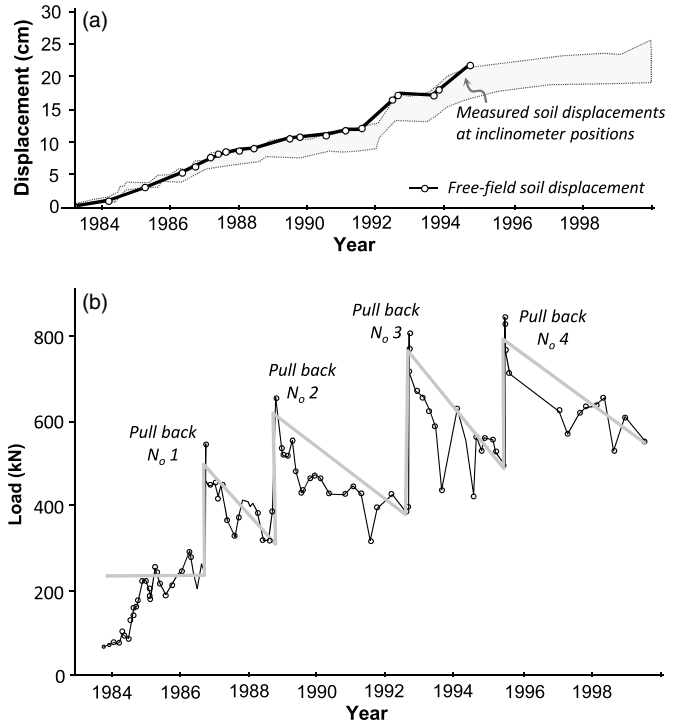


**Fig. 11.** Long-term full-scale field test by Frank and Pouget (2008): (a) measured evolution of soil displacements with time (gray shaded area) and free-field displacements time history (approximated by solid black line); (b) time history of pile-head force and approximation made for the numerical simulation (gray line)

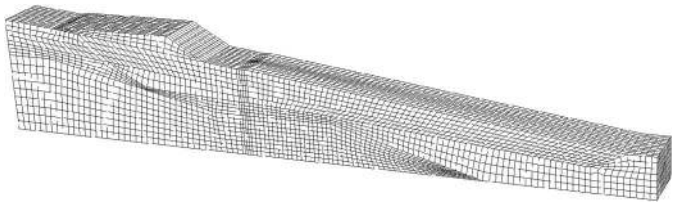

**Fig. 12.** Validation of numerical analysis method against long-term full-scale field test by Frank and Pouget (2008): finite-element discretization

**Comparison with 3D Finite-Element Analysis Results.** The field experimental setting was modeled numerically, utilizing the previously described FE modeling technique. The FE discretization is depicted in Fig. 12. The soil properties documented by Frank and Pouget (2008) were directly adopted without any calibration attempts.

In the field, the interface properties changed seasonally, resulting in soil movements and thereby pile deformation. In the present analysis, the shear strength of the interface is reduced until the onset of failure. This is achieved through a user subroutine that defines the strength-reduction pattern.

Frank and Pouget (2008) provide the time history of free-field soil displacements attributable to the fluctuation of soil strength caused by the fluctuation of water table. This fluctuation was actually the cause of the slope movement. Because no data as to the seasonal variation of the interface strength were available, the latter was obtained indirectly as follows: first, the time scale of the free-field displacement time history [Fig. 11(a)] was converted from 16 years to analysis steps. Hence, each year of the experiment represents 1/16 of the analysis step time. Second, a user-defined subroutine was introduced in ABAQUS to modify the soil strength during the time step. Several analyses were conducted to calibrate the fluctuation of soil strength within each time step (i.e., the user-defined subroutine) so that the produced free-field displacement time history is correctly compared to the measured one. If this calibration had been omitted and constant reduction of the strength had been assumed, the produced soil-displacement pattern at free-field would have monotonically increased constantly, unlike the observed reality. The analyses have been conducted using the free-field model (Fig. 12), i.e., the slope without any pile, so that the actual free-field conditions could be captured. The calibration results (Fig. 13) confirm the validity of the process. A similar conversion was employed for the time scale of the deadman-anchor force time history.

The deadman-anchor force was modeled as a concentrated force on the pile head. In the actual case, the anchor was pulled back as soon as the pile had deflected substantially at its top. The time history of the anchor horizontal force [as approximated by the gray curve in Fig. 11(b)] has been combined with the corresponding free-field soil-displacement time history [the black line in Fig. 11(a)] in order to correlate the horizontal force on the pile head with the soil displacement at the free field [Fig. 14]. The latter was then converted to force versus step time. Hence, soil

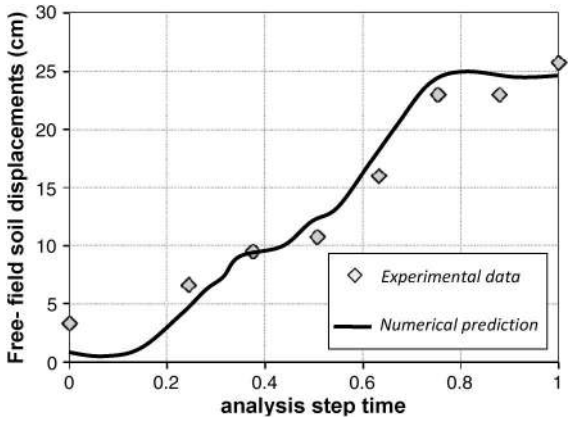


**Fig. 13.** Validation of numerical analysis method against long-term full-scale field test by Frank and Pouget (2008): FE-computed free-field soil displacement (plotted versus analysis step time) compared with experimental data

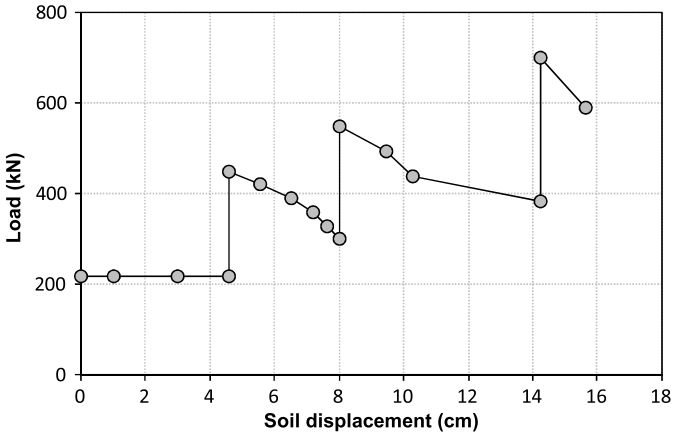


**Fig. 14.** Pile-head force versus soil free-field displacement assumed in the numerical analysis

displacement and anchor force have been converted to match the analysis step time scale, and could therefore be readily imposed on the FE model.

The aforementioned data were used to model the sequence of : (1) pile loading, (2) pile-head deflection, and (3) anchor pull-back. The 3D model with the pile and the slope was utilized. The external loads acting on the model are the gravity and the converted time history of anchor force, whereas the interface strength parameters fluctuate according to the user subroutine discussed previously.

The produced pile-deflection curve before and after each anchor pulling is plotted in Fig. 15 and compared with the Frank and Pouget (2008) field measurements at various stages of the anchor pullback. Obviously, before each jacking, the pile displacement is maximum at the pile head, whereas after jacking the pile displacement is greatest in its middle part because of soil thrust. The overall model performance in predicting the in situ slope (Fig. 13) and pile

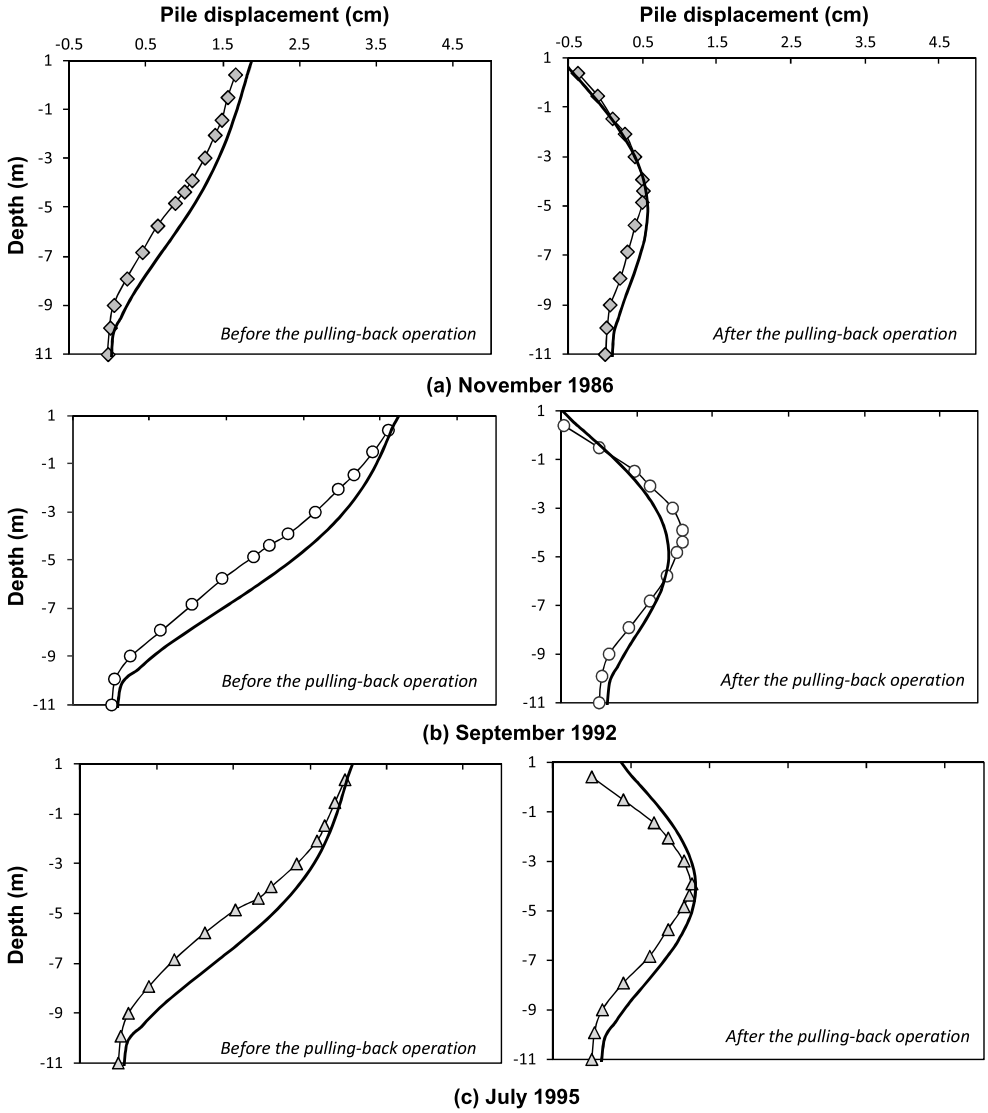


**Fig. 15.** Validation of numerical method against long-term full-scale field test by Frank and Pouget (2008): (a) pile displacements before (left) and after (right) the first pulling-back operation in November 1986; (b) pile displacements before (left) and after (right) the second pulling-back operation in September 1992; and (c) pile displacements before (left) and after (right) the third pulling-back operation in July 1995; black line denotes the numerical analysis results, and pile measurements of Frank and Pouget (2008) are denoted with distinct markers

(Fig. 15) displacements is quite satisfactory, adding to confidence in its validity.

**Verification against Theoretical Solutions.** Fig. 16(a) shows the mechanism of resistance-force development as the pile is subjected to uniform displacement $u_s$. The soil displacement forces the pile to deform, reaching a head displacement $u_p$ at which $u_p < u_s$. Therefore, the pile can be thought of as moving by $u = u_s - u_p$ at a direction opposite to the soil movement, which

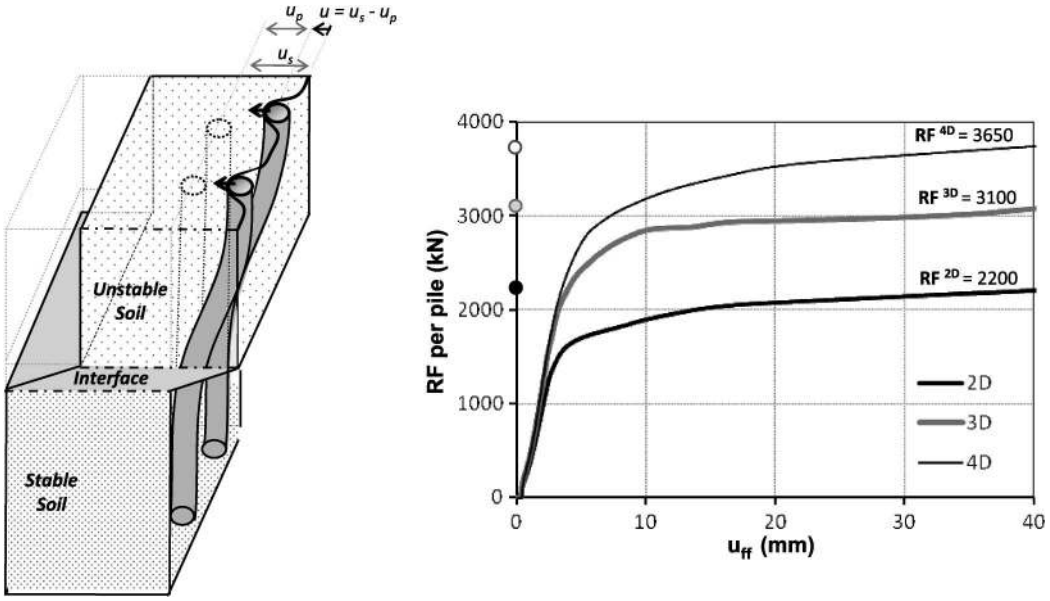


**Fig. 16.** Validation of numerical analysis against theoretical solutions: (a) schematic representation of the resistance-force development mechanism by piles embedded in slopes (the pile displaces $u_p < u_s$, i.e., resulting in mobilization of passive resistance); (b) resistance force developed on each pile as a function of free-field displacement

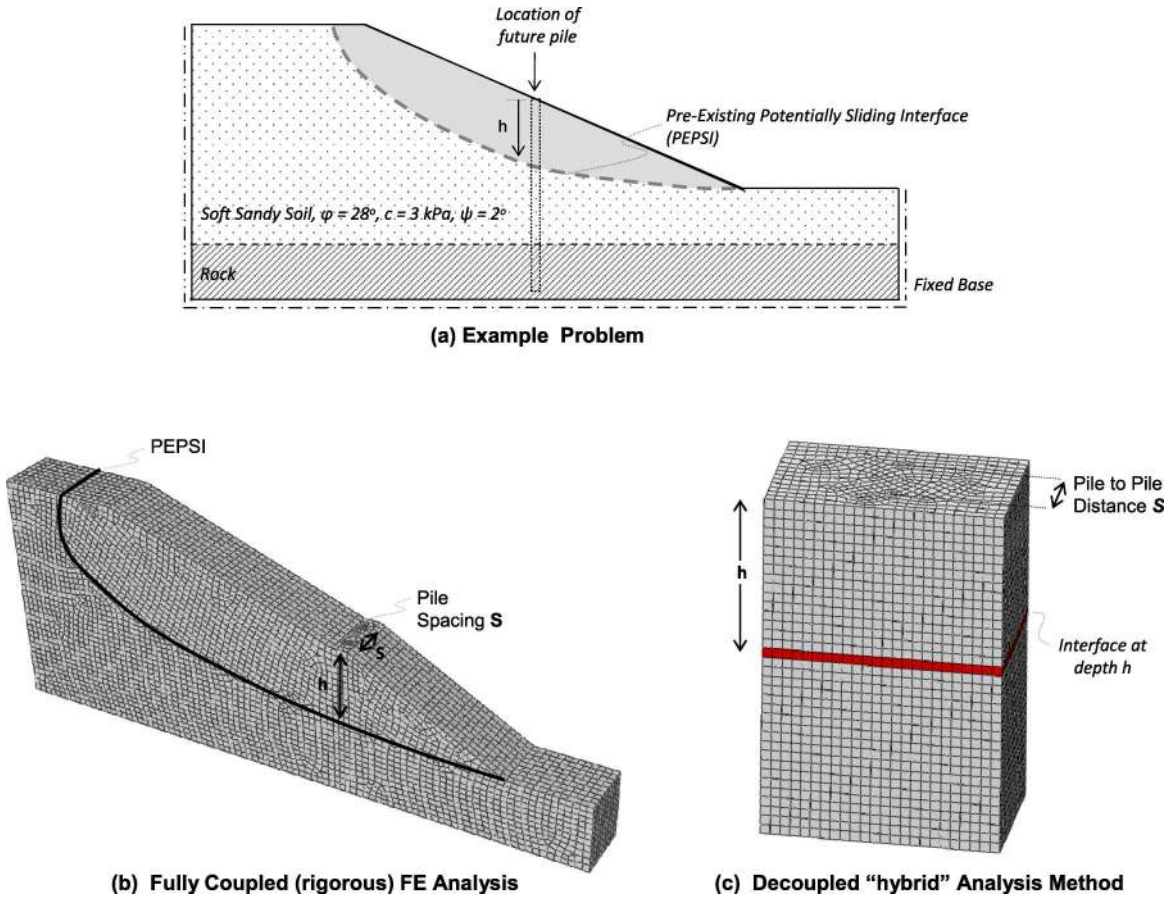


**Fig. 17.** Investigation of the validity of the proposed hybrid design method: (a) example problem; (b) FE mesh of the coupled 3D FE analysis; and (c) FE mesh of the decoupled hybrid analysis method

corresponds to the mechanism of passive resistance (the pile pushes into the soil). The ultimate lateral soil pressure, adopting the Broms 1964 lower-bound formula, is

$$P_u \approx 3\tan^2\left(45+\frac{\varphi}{2}\right)\sigma'_{vo} \quad (4)$$

Therefore, the theoretically calculated ultimate pile resistance is

$$RF \approx 3\tan^2\left(45+\frac{\varphi}{2}\right)D\frac{1}{2}\gamma z^2 \quad (5)$$

For an example case of $z = 6$ m and $D = 1.2$ m, $RF = 3{,}590$ kN.

The lateral pile capacity can be calculated by the finite-element method, utilizing the previously discussed simplified model. The plot of resistance force $RF$ developed per pile (and not per unit width) versus soil free-field displacement for the case of a shallow slide ($H_u = 6$ m) in sand stabilized by piles is displayed in Fig. 16(b) for three different values of the pile spacing $s$. The ultimate value ($RF_{\text{ult}}$) of the resistance force is clearly indicated by the attained plateau (displacements keep increasing, whereas the resistance force remains constant).

The value of the ultimate pile resistance force calculated for the three cases is as follows: for $s = 4D$, $RF_{\text{ult}} = 3{,}650$ kN$\approx$ $RF_{\text{Broms}} = 3{,}590$ kN; whereas for $s = 3D$, $RF_{\text{ult}} = 3{,}100$ kN; and for $s = 2D$, $RF_{\text{ult}} = 2{,}200$ kN.

Evidently, $RF_{\text{ult}}$ for closely spaced piles ($s \le 3D$) deviates substantially from the theoretical solution of Broms (1964). This is because of the group-interaction effect caused by the presence of neighboring piles. Other theoretical studies (Prakash 1962; Cox et al. 1984; Wang and Reese 1986; Liang and Zeng 2002; Liang and Yamin 2009) reveal that as the pile spacing decreases, the interference from adjacent piles reduces the passive resistance capacity of the pile compared with that of single piles. For axis-to-axis spacing $S$ and pile diameter $D$, the ultimate resistance force developed in each pile of a row of contiguous piles (i.e., $S/D = 1$) is only $1/3$ of that developed on a single isolated pile. [For clay materials under undrained conditions, this increases to $1/2$ (Wang and Reese 1986).] The difference between piles in a group and single piles becomes less significant when the $S/D$ ratio is between 3 and 4, and is diminished when the ratio exceeds 5.

Hence, in full accord with theoretical considerations, the FE analysis reveals that the $RF_{\text{ult}}$ value calculated for piles spaced at $4D$ best matches the theoretical $P_u$ value. For piles spaced at $2D$, $RF_{\text{ult}}$ is almost 60% of the single-pile lateral capacity (i.e., 3,650 kN), increasing to approximately 85% for piles spaced at $3D$.

A similar comparison was conducted for a clay with undrained shear strength $S_u$. In this case, the pile ultimate lateral capacity calculated by FE analysis was $RF_{\text{ult}} = 11.2S_uD$ for piles spaced at $4D$, whereas for closely spaced piles (at $2D$) $RF_{\text{ult}} = 9S_uD$. These results are also in accord with the theoretical solution of Poulos (1999).

## Illustration of Validity of Proposed Design Method

Having validated the numerical aspect of the methodology, the validity of the whole proposed hybrid design method can now be demonstrated (Fig. 17). A number of typical slope geometries and pile configurations are analyzed by means of both the coupled and the uncoupled methodology, and the results are comparatively discussed.

### Fully Coupled Analysis of Slope-Stabilization Piles

The validated numerical procedure was adopted to conduct 3D coupled analyses for a number of cases, summarized in Table 1. These refer to mild homogeneous slopes of 20–24° inclination. The bottom stable layer, starting 10 m below the toe of the slope, is assumed to be rock. The top layer is a typical, relatively loose sandy soil with $\varphi = 28°$, $c = 3$ kPa, and $\psi = 2°$. A preexisting potential sliding interface (PEPSI) is assumed, with strength properties gradually reducing from the initial values ($\varphi = 28°$, $c = 3$ kPa, and $\psi = 2°$) to their residual properties shown in Table 1.

The initial safety factor is of the order of two; hence, failure may only occur along the interface once its strength parameters have

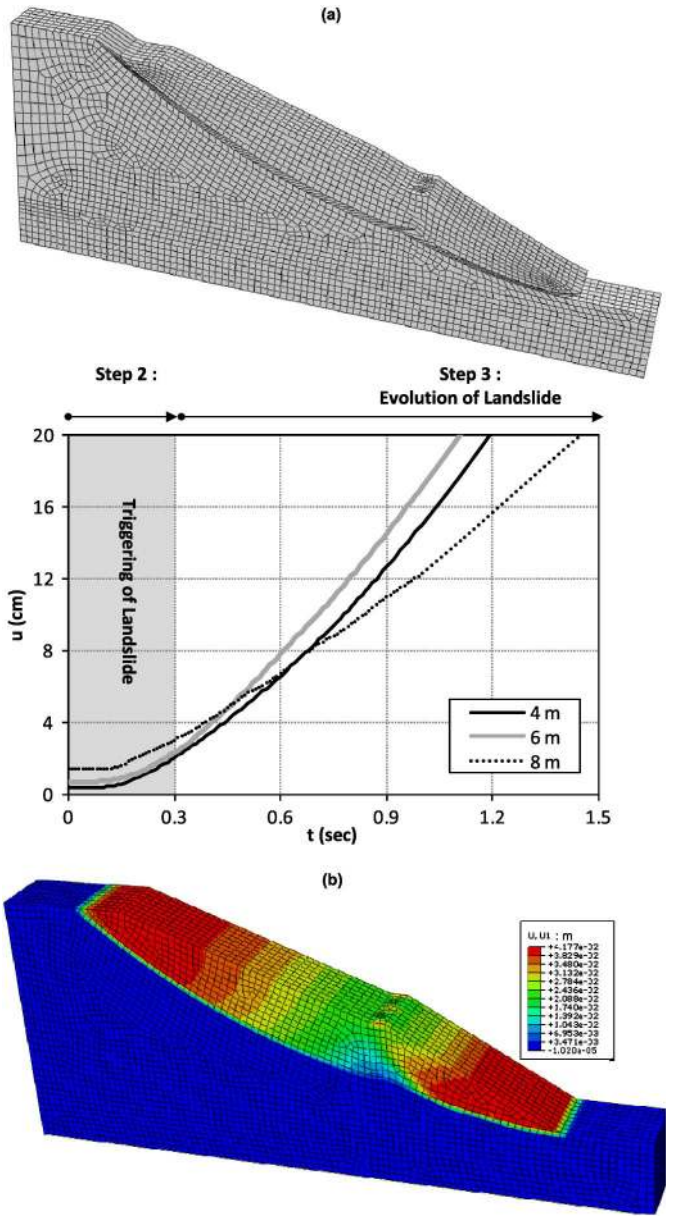


**Fig. 18.** Analysis of typical example problems through fully coupled 3D FE approach: (a) free-field analysis (no piles installed) showing snapshot of deformed mesh (for a 6 m landslide, slope inclination $\beta = 22°$) and time histories of soil displacement within the sliding wedge (on a node located 2 m upslope of the pile row) for all examined landslide depths; (b) contours of horizontal soil displacements when slope-stabilizing piles have been installed

been reduced, dropping the safety factor well below unity. The landslide depth in the middle of the slope (where the piles are located) varies parametrically from 4 to 8 m. The interface geometry is almost circular and in all cases examined, the soil block downslope from the piles location is stable (i.e., it is not prone to failure if the upper part of the slope has been stabilized). Single rows of piles of 1.2-m diameter, spaced at two and three diameters, are employed for the stabilization of the slopes.

The fully coupled 3D FE model is displayed in Fig. 18(b). An initial analysis is performed in free-field conditions; i.e., without any stabilization piles installed [Fig. 18(a)]. The numerical analysis is performed in three consecutive steps: (1) gravity loading (static analysis), during which the initial state of stress in the slope is established; (2) triggering of the landslide (analysis in the time domain), during which the strength in the predetermined sliding interface is greatly reduced (a parametric analysis showed that the problem is not sensitive to the duration of this step); and (3) evolution of the slide (analysis in the time domain), a continuation of the previous step without any further strength reduction. As shown in Fig. 18(a), at the end of the analysis the unstable soil mass slides

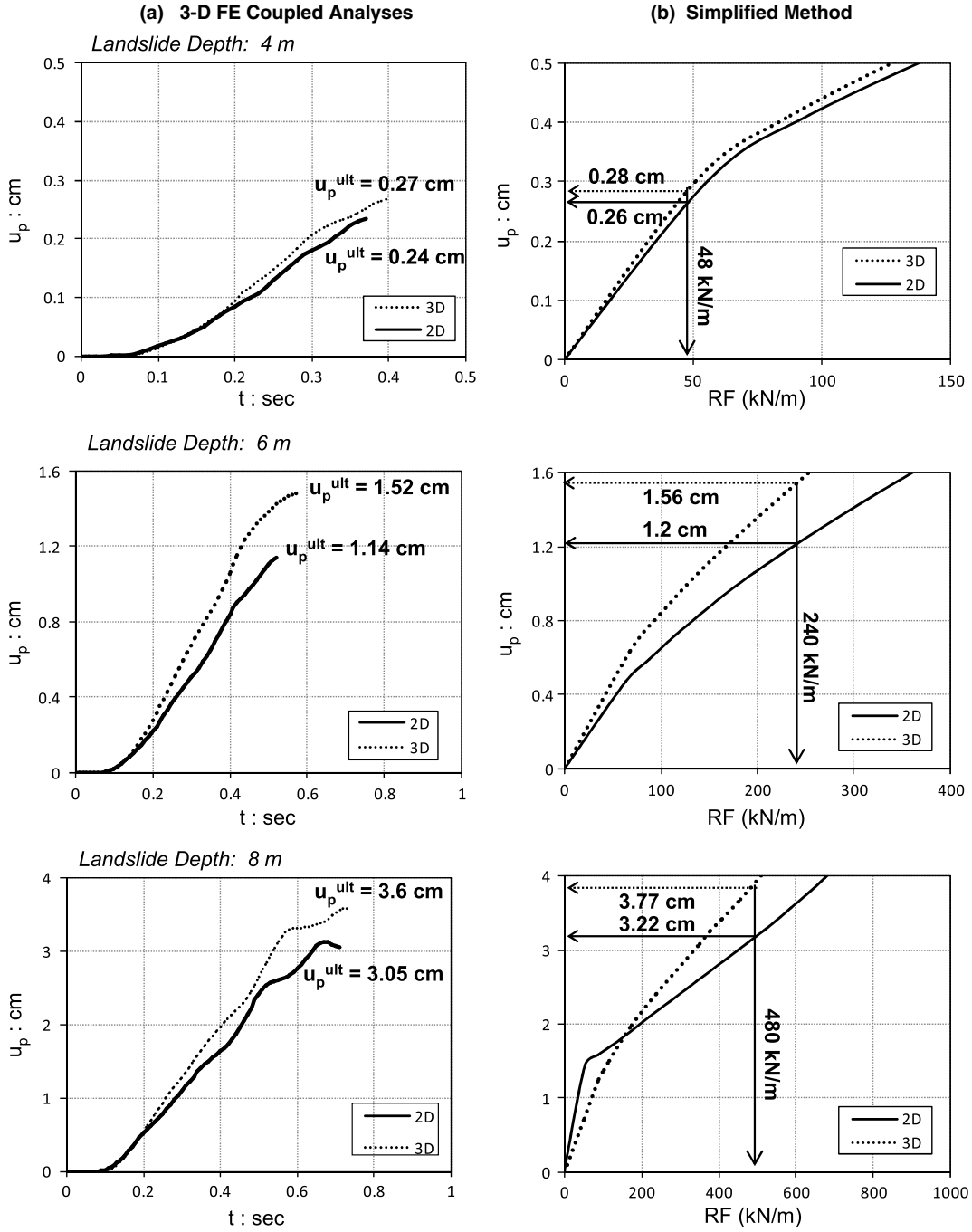


**Fig. 19.** Illustration of the validity of the proposed hybrid design method for pile spacings 2*D* (solid black line) and 3*D* (dotted black line) and landslide depths from 4 m (case of a relative shallow landslide) to 8 m (relative deep landslide): (a) time history of pile-head displacements computed with the coupled analysis; (b) *RF* versus pile-head displacement as calculated by using the simplified numerical model; the ultimate value of the pile deflection from the coupled analysis is compared with the required pile deflection to provide the necessary resisting force per running width, utilizing the proposed hybrid methodology

**Table 2.** Comparison of Pile-Head Deflection Necessary to Stabilize Slopes by Both Coupled and Simplified Methodology

| Slope inclination ($\beta$°) | Interface depth (m) | Required $RF$(kN/m; calculated by the 2D slope geometry) | Pile-to-pile distance | Full 3D analyses $u_p$ at pile head (cm) | Decoupled methodology $u_p$ at pile head (cm) | Error (%) |
|---|---|---|---|---|---|---|
| | | Residual interface strength properties: $\varphi = 19°$, $c = 3$ kPa | | | | |
| 24 | −8 | 480 | 2$D$ | 3.05 | 3.22 | 5.57 |
| | | | 3$D$ | 3.6 | 3.77 | 4.72 |
| | | Residual interface strength properties: $\varphi = 16°$, $c = 3$ kPa | | | | |
| 22 | −6 | 240 | 2$D$ | 1.14 | 1.2 | 5.26 |
| | | | 3$D$ | 1.52 | 1.56 | 2.63 |
| | | Residual interface strength properties: $\varphi = 14°$, $c = 3$ kPa | | | | |
| 20 | −4 | 48 | 2$D$ | 0.24 | 0.26 | 8.33 |
| | | | 3$D$ | 0.27 | 0.28 | 3.70 |

along the predetermined slip surface with increasing velocity, implying complete (i.e., catastrophic) slope failure for all cases examined.

Having confirmed the potential instability of the slope for the residual strength of the sliding interface, the analysis is repeated with the presence of slope-stabilizing piles. As witnessed by the contours of soil displacement after the end of the analyses [Fig. 18(b)], the chosen pile configuration has effectively stabilized the slope; the maximum soil displacement does not exceed 5 cm for the worst-case scenario. The time histories of horizontal deflection of the pile head that produce the required stabilization force are plotted in Fig. 19(a).

### *Analysis of Slope-Stabilization Piles Applying the Proposed Hybrid Decoupled Methodology*

The same cases were also examined using the design charts produced by the decoupled approach:

**Step 1: Calculation of Required Lateral Resisting Force to Be Offered by Piles.** Assuming residual properties at the interface, the pile resisting force (per unit width) required to raise the slope safety factor to unity is calculated by subtracting the resisting forces from the driving forces.

**Step 2. Estimation of Pile Configuration to Provide the Required RF at Acceptable Deflection.** Having estimated the required resisting force, $RF$, per slope unit width to be offered by piles, the simplified method for estimation of pile ultimate resistance is utilized. Following the previously discussed methodology, a simplified decoupled model is developed for the specific pile configuration [Fig. 17(c)]. The model is subjected to horizontal displacement $u_{ff}$. An initial free-field (i.e., without piles) analysis is performed to obtain the soil shear resistance at the interface. The analysis is then repeated with the piles to compute the net resisting force. Such analyses produce design charts for the case under consideration, as discussed previously. The design charts produced for the examples analyzed in this section ($RF$ versus pile-head deflection) are displayed in Fig. 19(b).

The results of the two methods are compared in Table 2. The pile deflection at the instant when the sliding has ceased is compared to the deflection necessary for the same pile configuration to offer the required $RF$, as calculated by the decoupled design charts. The decoupled approach slightly overpredicts the necessary pile deflection compared to the rigorous coupled method. This may be attributed to the conservatism included in the calculation of the required $RF$ using conventional slope-stability analysis. However, the error computed in the calculation of pile deflection for the cases examined is invariably much less than 10%.

## Summary and Conclusions

This paper has presented a hybrid methodology for the design of slope-stabilizing piles. The method combines the rigor of 3D finite-element simulation with the simplicity of widely accepted analytical techniques. Following the well-documented decoupled approach (Viggiani 1981; Hull 1993; Poulos 1995, 1999), the procedure involves two steps: (1) evaluation of the required lateral resisting force, $RF$, needed to increase the safety factor of the slope to the desired value, and (2) estimation of pile configuration that offers the required $RF$ for a prescribed deformation level.

The first step uses the results of conventional slope-stability analysis and may be readily applied by engineering practitioners. Aimed at reducing the amount of computational effort usually associated with rigorous 3D soil-structure interaction analyses, a new approach is proposed for computation of pile lateral capacity (Step 2). The key ingredient of the method lies in decoupling the slope-geometry effect from the calculation of pile lateral capacity, which allows numerical modeling of only a limited region of soil around the piles. The method is especially applicable to cases of preexisting potential sliding interfaces within slopes; the possible modification of the interface position caused by the presence of piles is not taken into account.

The numerical methodology employed in this paper was thoroughly validated against published experimental (centrifuge and 1-$g$ tests), field (a long-term, large-scale experiment), and theoretical solutions. The validity of the hybrid decoupled approach was demonstrated through comparisons with fully coupled 3D nonlinear finite-element analysis.

The proposed simplified method for estimation of pile lateral capacity provides a computationally efficient tool that can be utilized for parametric analyses and design. The methodology presented in this paper is further exploited in Kourkoulis et al. (2011) to gain further insight into the factors affecting the response and to produce practically useful design charts for slope-stabilization piles.

## Acknowledgments

This work was partially supported by the European Union Seventh Framework Research Project, funded through the European Research Council (ERC) Ideas Programme, in support of Frontier Research Advanced Grant (contract number ERC-2008-AdG 228254-DARE).

## References


*ABAQUS FEA* [Computer software]. D. S. Simulia, Dassault Systémes.

Ambraseys, N., and Srbulov, M. (1995) "Earthquake induced displacements of slopes." *Soil Dyn. Earthquake Eng.*, 14(1), 59–72.

Broms, B. (1964). "Lateral resistance of piles in cohesionless soils." *J. Soil Mech. Found. Div.*, 90(SM3), 123–156.

Cai, F., and Ugai, K. (2000). "Numerical analysis of the stability of a slope reinforced with piles." *Soils Found.*, 40(1), 73–84.

Chandler, R. J. (1984). "Recent European experience in landslides in overconsolidated clays and soft rocks." *Proc., 4th Int. Symp. on Landslides*, Vol. 2, University of Toronto Press, Toronto, Canada, 19–25.

Chen, L. T., and Poulos, H. G. (1993). "Analysis of pile-soil interaction under lateral loading using infinite and finite elements." *Comput. Geotech.*, 15(4), 189–220.

Chen, L. T., Poulos, H. G., and Hull, T. S. (1997). "Piles subjected to lateral soil movements." *J. Geotech. Geoenviron. Eng.*, 123(9), 802–811.

Chow, Y. K. (1996). "Analysis of piles used for slope stabilization." *Int. J. Numer. Anal. Meth. Geomech.*, 20(9), 635–646.

Cox, W. R., Dixon, D. A., and Murphy, B. S. (1984). "Lateral load tests of 5.4 mm diameter piles in very soft clay in side-by-side and in-line groups." *Laterally loaded deep foundations: Analysis and performance*, ASTM, West Conshohocken, PA.

D'Appolonia, E., Alperstein, R., and D'Appolonia, D. J. (1997). "Behavior of colluvial slope." *J. Soil Mech. Found. Div.*, 93(SM4), 447–473.

De Beer, E. E., and Wallays, M. (1972). "Forces induced in piles by unsymmetrical surcharges on the soil round the piles." *Conf. on Soil Mechanics and Foundation Engineering*, Vol. 1, Spanish Society for Soil Mechanics and Foundations, Madrid, Spain, 325–332.

Frank, R., and Pouget, P. (2008). "Experimental pile subjected to long duration thrusts owing to a moving slope." *Géotechnique*, 58(8), 645–658.

Fukuoka, M. (1977). "The effects of horizontal loads on piles due to landslides." *Proc., 9th Int. Conf. on Soil Mechanics and Foundation Engineering*, Japanese Society of Soil Mechanics and Foundation Engineering, Tokyo, 27–42.

Gazetas, G., and Uddin, N. (1994). "Permanent deformation of preexisting sliding surfaces in dams." *J. Geotech. Eng.*, 120(11), 2041–2061.

Goh, A. T. C., The, C. I., and Wong, K. S. (1997). "Analysis of piles subjected to embankment induced lateral soil movements." *J. Geotech. Geoenviron. Eng.*, 123(4), 312–323.

Guerpillon, Y., Boutonnier, L., Gay, O., Foray, P., and Flavigny, E. (1999). "Modelisation phisique et numerique de l'interaction d'un obstacle et d'un glissement d'epaisseur limitee." *Proc., 12th European Conf. on Soil Mechanics And Foundation Engineering*, A. A. Balkema, Rotterdam, Netherlands.

Hassiotis, S., Chameau, J. L., and Gunaratne, M. (1997). "Design method for stabilization of slopes with piles." *J. Geotech. Geoenviron. Eng.*, 123(4), 314–323.

Heyman, L., and Boersma, L. (1961). "Bending moment in piles due to lateral earth pressure." *Proc., 5th Int. Conf. on Soil Mechanics and Foundation Engineering*, Vol. 2, Durod, Paris, 425–429.

Hull, T. S. (1993). "Analysis of the stability of slopes with piles." *11th Southeast Asian Geotechnical Conf.*, Southeast Asian Geotechnical Society, Bangkok, Thailand, 639–643.

Ito, T., and Matsui, T. (1975). "Methods to estimate lateral force acting on stabilizing piles." *Soils Found.*, 15(4), 43–60.

Jeong, S., Kim, B., Won, J., and Lee, J. (2003). "Uncoupled analysis of stabilizing piles in weathered slopes." *Comput. Geotech.*, 30(8), 671–682.

Kim, J., Salgado, R., and Lee, J. (2002). "Stability analysis of complex soil slopes using limit analysis." *J. Geotech. Geoenviron. Eng.*, 128(7), 546–557.

Kitazima, S., and Kishi, S. (1967). "An effect of embedded pipes to increase resistance against circular slides in soft clay foundation." *Technical note of Port and Harbour Research Institute*, Vol. 29, Ministry of Transport, Japan, 63–94 (in Japanese).

Kourkoulis, R. (2009). "Interplay of mat foundations and piles with a failing slope." Ph.D. thesis, National Technical Univ. of Athens, Athens, Greece.

Kourkoulis, R., Gelagoti, F., Anastasopoulos, I., and Gazetas, G. (2011). "Slope stabilizing piles and pile-groups: Parametric study and design insights." *J. Geotech. Geoenviron. Eng.*, 137(7), 663–678.

Leussink, H., and Wenz, K. P. (1969). "Storage yard foundations on soft cohesive soils." *Proc., 7th Int. Conf. on Soil Mechanics and Foundation Engineering*, Vol. 2, Sociedad Mexicana de Mecanica de Suelos, Mexico City, 149–155.

Liang, R. Y., and Yamin, M. M. (2009). "Three-dimensional finite element study of arching behavior in slope/drilled shafts system." *Int. J. Numer. Anal. Methods Geomech.*, 34(11), 1157–1168.

Liang, R. Y., and Zeng, S. (2002). "Numerical study of soil arching mechanism in drilled shafts for slope stabilization." *Soils Found.*, 42(2), 59.

Nethero, M. F. (1982). "Slide control by drilled pier walls." *Application of Walls to Landslide Control Problems: Proc., ASCE National Convention*, R. B. Reeves, ed., ASCE, New York, 19–29.

Nicu, N. D., Antes, D. R., and Kesslerr, S. (1971). "Field measurements on instrumented piles under an overpass abutment." *Highway Research Record 354*, Highway Research Board, Washington, DC.

Oakland, M. W., and Chameau, J. L. A. (1984). "Finite-element analysis of drilled piers used for slope stabilization." *Laterally loaded deep foundations*, ASTM, West Conshohoken, PA, 182–193.

Popescu, M. E. (1991). "Landslide control by means of a row of piles." *Slope Stability Engineering: Proc., Int. Conf. on Slope Stability*, Thomas Telford, London, 389–394.

Poulos, H. G. (1973). "Analysis of piles in soil undergoing lateral movement." *J. Soil Mech. Found. Div.*, 99(SM5), 391–406.

Poulos, H. G. (1995). "Design of reinforcing piles to increase slope stability." *Can. Geotech. J.*, 32(5), 808–818.

Poulos, H. G. (1999). "Design of slope stabilizing piles." *Slope stability engineering*, N. Yagi, T. Yamagami, and J. C. Jiang, eds., A. A. Balkema, Rotterdam, Netherlands.

Poulos, H. G., and Chen, L. T. (1997). "Pile response due to excavation-induced lateral soil movement." *J. Geotech. Geoenviron. Eng.*, 123(2), 94–99.

Prakash, S. (1962) "Behavior of pile groups subjected to lateral loading." Ph.D. thesis, Univ. of Illinois, Urbana, IL.

Reese, L. C., and Van Impe, W. F. (2001). *Single piles and pile groups under lateral loading*, A. A. Balkema, Rotterdam, Netherlands, 463.

Reese, L. C., Wang, S. T., and Fouse, J. L. (1992). "Use of drilled shafts in stabilizing a slope." *Proc., Specialty Conf. on Stability and Performance of Slopes and Embankments II (GSP 31)*, Vol. 2, ASCE, New York, 1318–1332.

Rowe, R. K., and Poulos, H. G. (1979). "A method for predicting the effect of piles on slope behaviour." *Proc., 3rd Int. Conf. on Numerical Methods in Geomechanics*, Vol. 3, A. A. Balkema, Rotterdam, Netherlands, 1073–1085.

Sommer, H. (1977). "Creeping slope in a stiff clay." *Proc., 9th Int. Conf. on Soil Mechanics and Foundation Engineering*, A. A. Balkema, Rotterdam, Netherlands, 113–118.

Tika-Vassilikos, T., Sarma, S., and Ambraseys, N. (1993) "Seismic displacements on shear surfaces in cohesive soils." *Earthquake Eng. Struct. Dyn.*, 22(8),709–721.

Tschebotarioff, G. P. (1973). *Foundations, retaining and earth structures*, McGraw Hill, New York.

Viggiani, C. (1981). "Ultimate lateral load on piles used to stabilize landslides." *Proc., 10th. Int. Conf. on Soil Mechanics and Foundation Engineering*, Vol. 3, A. A. Balkema, Rotterdam, Netherlands, 555–560.

Wang, M. C., Wu, A. H., and Scheessele, D. J. (1979). "Stress and deformation in single piles due to lateral movement of surrounding soils." *Behavior of deep foundations: ASTM special technical publication*, Vol. 670, Raymond Lunggren, ed., ASTM, West Conshohocken, PA, 578–591.

Wang, S. T., and Reese, L. C. (1986). "Study of design method for vertical drilled shaft retaining walls." *Research Rep. 415-2F*, Univ. of Texas Center for Transportation Research, Austin, TX.

Yamin, M., and Liang, R. Y. (2009). "Limiting equilibrium method for slope/drilled shaft system." *Int. J. Numer. Anal. Methods Geomech.*, 34(10), 1063–1075.

Zeng, S., and Liang, R. Y. (2002). "Stability analysis of drilled shafts reinforced slope." *Soils Found.*, 42(2), 93–102.